



Alexandria University
Alexandria Engineering Journal

www.elsevier.com/locate/aej
www.sciencedirect.com



Mixed convective thermal transport in a lid-driven square enclosure with square obstacle

Noor Zeb Khan ^a, Rashid Mahmood ^a, Sardar Bilal ^a, Ali Akgül ^{b,i,*},
 Sherzod Abdullaev ^c, Emad E. Mahmoud ^d, Ibrahim S. Yahia ^{e,f,g}, Choonkil Park ^{h,*}

^a Department of Mathematics, Air University, P.A.F Complex E-9, Islamabad 44000, Pakistan

^b Siirt University, Art and Science Faculty, Department of Mathematics, 56100 Siirt, Turkey

^c Independent Researcher and CEO of the Company “Editory” LTD, Independent Researcher, Andijan Machine-Building Institute, Uzbekistan

^d Department of Mathematics and Statistics, College of Science, Taif University, PO Box 11099, Taif 21944, Saudi Arabia

^e Department of Physics, Faculty of Science, King Khalid University, P.O. Box 9004, Abha 61413, Saudi Arabia

^f Research Center for Advanced Materials Science (RCAMS), King Khalid University, P.O. Box 9004, Abha 61413, Saudi Arabia

^g Nanoscience Laboratory for Environmental and Biomedical Applications (NLEBA), Metallurgical Laboratory 1, Department of Physics, Faculty of Education, Ain Shams University, Roxy, Cairo 11757, Egypt

^h Research Institute for Natural Sciences, Hanyang University, Seoul 04763, Republic of Korea

ⁱ Near East University, Mathematics Research Center, Department of Mathematics, Near East Boulevard, PC: 99138, Nicosia /Mersin 10 – Turkey

Received 14 April 2022; revised 16 August 2022; accepted 22 August 2022

KEYWORDS

Mixed convection;
 Power law fluid;
 Square cavity;
 Square cylinder (Adiabatic and Cold);
 Non-uniform and uniform heating

Abstract The prime motive of this disquisition is to scrutinize simultaneous aspects of external forcing mechanism and internal volumetric forces on non-Newtonian liquid filled in square enclosure. Inertially driven upper lid is assumed by providing constant magnitude of slip velocity whereas thermal equilibrium is disturbed by assuming uniform temperature at lower boundary and by keeping rest of walls as cold. To enhance thermal diffusion transport with in the flow domain cold as well as adiabatic temperature situation is provided. In view of velocity constraints all the extremities at no-slip except the upper wall which is moving with U_{Lid} . Formulation is attained in dimensional form initially and afterwards variables are used to convert constructed differential system into dimensionless representation. A numerical solution of leading formulation is sought through Galerkin finite element discretization. Momentum and temperature equations are interpolated by quadratic polynomials whereas pressure distribution is approximated by linear interpolating function. Domain discretized version is evaluated in view of triangular and rectangular elements. Newton’s scheme is employed to resolve the non-linearly discretized system and a matrix factorization based non-linear solver renowned as PARADISO is used. Validation of results is ascertained by forming agreement with existing studies. In addition, grid independence test is also performed to show

* Corresponding authors.

E-mail addresses: aliakgul00727@gmail.com (A. Akgül), baak@hanyang.ac.kr (C. Park).

Peer review under responsibility of Faculty of Engineering, Alexandria University.

<https://doi.org/10.1016/j.aej.2022.08.031>

1110-0168 © 2022 THE AUTHORS. Published by Elsevier BV on behalf of Faculty of Engineering, Alexandria University.

This is an open access article under the CC BY-NC-ND license (<http://creativecommons.org/licenses/by-nc-nd/4.0/>).

Please cite this article in press as: N.Z. Khan et al., Mixed convective thermal transport in a lid-driven square enclosure with square obstacle, Alexandria Eng. J. (2022), <https://doi.org/10.1016/j.aej.2022.08.031>

credibility of performed computations. Stream lines and isothermal contours patterns are portrayed to evaluate variation in flow distributions. Kinetic energy and local heat flux for uniform and non-uniform heating situations are also divulged in graphical and tabular formats. Increase in Reynold number produces decrease in kinetic energy of fluid. Enhancement in Grashof number causes enrichment of thermal buoyancy forces due to which Nusselt number uplifts. Clock wise rotations increase against upsurge in magnitude of Reynold number which is evidenced form stream lines. Squeezing of secondary vortex against Prandtl number arises due to dominance of viscous forces.

© 2022 THE AUTHORS. Published by Elsevier BV on behalf of Faculty of Engineering, Alexandria University. This is an open access article under the CC BY-NC-ND license (<http://creativecommons.org/licenses/by-nc-nd/4.0/>).

1. Introduction

Momentum and thermal diffusivities produce by inertial movement of lid in enclosures are major effective parameters in mixed convection. Due to advancement in technologies and highly needed demand for elevated energy production researchers have propagated various techniques. Among these approaches are of the successful procedure specifically in closed domain in the joint consideration of inertial and buoyant forces. Because when flow is induced by external agent or by providing velocity at boundary the temperature difference between the solid surface and fluid layers causes decrease in the density of fluid particles upward and descend the heavy particles. The generated fluid movement results elevation in thermal transport with computational domain according to researchers, the aforementioned technique is considered as an efficient alternative way instead of performing experimentation regarding rise in thermal characteristics in enclosure due to less time and monitory consumption. In present work we have aimed to explore and report numerical studies regarding mixed convection thermal transport. Pragmatic significance of combined free and forced convection is entrenched in numerous industries and frameworks like food and glass production industries, electronic industry (cooling electronic devices), power generators, cooling towers, resin transfer moulding, fiber composite manufacturing, aerosol filters, electronic equipment's and so many [1–4]. The combined influence of these forces signifies in the situation when the forced flow is less effective than the temperature differences. In view of these characteristics such type of phenomenon is appeared in polymers manufacturing, paper productivity, drawing of wire, melt spinning, casting, wind-up rolling, metallic plate cooling, etc. [5–7]. In addition, mixed convection occurring in confined physical configurations possesses promising utilizations in geothermal energy extraction, underground storage systems, ventilation of buildings, annular tubes, heat reduction in reactors, gas turbines, automobile engines and atmospheric and oceanic flow. In view of such remarkable utilizations abundant investigations had been under taken for exploring concerned phenomenon like Basak et al. [8] implemented FEM to analyse momentum and thermal characteristics in mixed driven convective flow of viscous fluid in a square enclosure. They determined that transitional situation for conversion of natural to forced convection extensively depends on Grashof number irrespective of Prandtl number. They also deduced that Prandtl number has influential role in enhancing circulation cells generated due to provision of lid driven force. Nouar [9] investigated forced convection flow of laminarly streamed Newtonian liquid in an annular duct with constant heat flux density. He adopted Prandtl Boussinesq

hypothesis and formulated 3D parabolized system of differential equations comprising momentum and energy equations by solving finite differencing scheme. Bejan [10] executed scale analysis of mixed convective flow over a vertical surface to measure transitional range of Prandtl number for which forced convection dominates the natural convection phenomenon. They varied the magnitude of Prandtl number from small to moderate scale and calculated variation in local and average heat flux coefficients. Thermal attributes in lid driven cavity by performing experimentation for heat flux measurement at different location of heated base wall against Reynold (Re) and Grashof (Gr) numbers was manifested by Prasad and Koseff [11]. Mohammad and Viskanta [12] described instability in a shallow enclosure with movement of wall by placing heat source at base wall and depicted linear stability at initial of flow regime against Prandtl number (Pr). Amiri et al. [13] explicated mixed convective thermal transport in enclosure with sinusoidal distribution. They measured change in physical quantities like average Nusselt number against increase in undulation of wavy structure. Oztop and Dagtekin [14] probed steady 2D mixed convection in a vertically positioned cavity with installation of differentially heated sources. In this problem they maintained extremities in moving condition and adumbrated flow and heat transfer characteristic against different magnitude of Richardson number (Ri) which describe different convection regimes in the domain. Khanafer and Aithal [15] conducted computational analysis by executing finite element formulation to find heat transfer attributes in a lid-driven enclosure with placement of circular object. Some recent developments related to mixed convective heat transfer in different physical domains and constraints are accumulated in refs. [16–23].

Viscosity is the intrinsic attribute of materials which characterize the execution of interial resistance against shear. The fluids exhibiting non-variant aptitude in strain against applied force are classified as “Newtonian”. The basic natural component of life i.e. air and water without which survival of living objects is impossible are Newtonian in nature. Water is the compulsory requirement of life possess consistency in viscosity which make it more appropriate. In spite of thermally stratified environment water depicts Newtonian behaviour. In addition, viscous fluids play significant role in the removal of countenances in filtration, fuel consumption in engines, equipment testing, slurries and get formulation and so forth. Subsequently, the motion of viscous liquids along with temperature provision by convective forces may make them applicable and advantage in many disciplines. So here a vast wealth of knowledge and efforts on mixed convective flow of viscous liquid is presented. In literature extensive data is available regarding natural convective heat transmission in Newtonian fluids

which possess applications like in filtration screens, fuel elements of nuclear reactors, fluidized bed drying of fibrous materials, filtration of paper and pulp suspension, flow metering devices and in biological systems. Dazodzo and Dazodzo [24] described the effectiveness and demand of velocity and temperature distributions generated by natural convection in flow of ordinary (water and air) in liquid metal reactors and encapsulated nuclear heat source. Backermann et al. [25] executed numerical and experimental study to evaluate steady state natural convection in viscous fluid enclosed in a vertical enclosure saturated by porous medium. They concluded that for relatively low magnitude of Rayleigh number (Ra) and Prandtl number (Pr) the flow takes place in the fluid layer and heat transfer arises in the porous layer via conduction. Ali et al. [26] conducted computational study on natural convective heat transfer in viscous fluid embedded in non-Darcian rectangular enclosure by assuming moderate magnitude of Darcy and Rayleigh numbers. Physical insight about instability in creeping air flow in circular enclosure with centrally localized heating generator was deliberated by Torrance and Rockett [27]. Latest studies on free convective heat transfer in Newtonian fluid is encapsulated in refs. [28–37].

Convective heat transfer in water-based nanoparticles in a permeable enclosure by considering thermally localized non-equilibrium model along with installation heated solid cylinder and heated bottom wall was demonstrated by Alsabery et al. [38]. The probed influential aspect of particle volume fraction and variation undulation on heat transfer characteristics by measuring heat flux. Tayebi and Chamkha [39] executed numerically computation to analyse the thermo-physical features of naturally convective hybrid nano-liquid under the appliance of magnetized and entropy. Dogonchi and his co-workers [40–41] investigated natural convective heat transfer in enclosure by varying morphological aspects of instructed nano-particle in base fluid.

On the basis of available literature review, it is concluded that mixed convective heat transfer in liquid in enclosure has superb essence in modern research. In this regard, the aim of the present effort is to scrutinize momentum and heat transport mechanisms in flow domain due to provision of inertial and temperature gradient forces at the boundaries. So far, natural convection phenomenon in viscous fluids like water and air in enclosures is discussed but the description of rheological behaviour of Newtonian fluids with mixed convection is very sparse. Additionally, installation of cylinder in enclosures is extensively incorporated in wide range of engineering applications of civil and industrial environments, such as indoor energy management, cooling of shafts, lubrications of bearings and food processing. In enclosure thermal management is also controlled/enhanced by placing cylinder of diversifiable thermal distributions. The aim of this document is to fill this gap by providing comprehensive elucidation about heat transport generated by mixed convection in the flow of Newtonian (water) with placement of adiabatically natured square cylinder. The authors have hoped that this work will definitely provide direction and broad spectrum to investigators.

2. Mathematical modelling

Let us assume steady, incompressible flow of viscous liquid in 2D square enclosure as presented in Fig. 1. Aspects of inertial

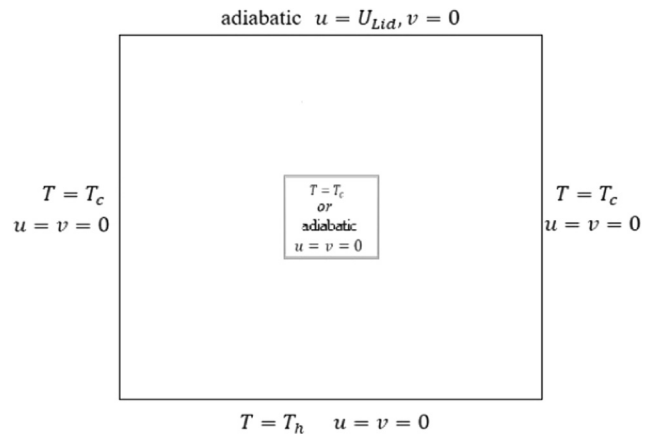


Fig. 1 Diagram for physical configuration.

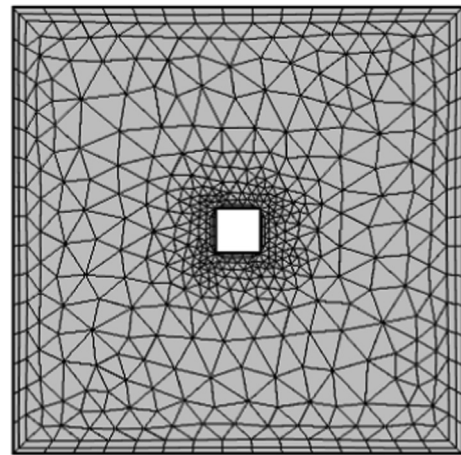


Fig. 2 Coarse grid for cavity with a square block placed at C (0.5,0.5).

Table 1 Mesh statistics for various refinement levels.

Lev	#EL	#DOFs
1	302	2442
2	500	3892
3	830	5910
4	1476	10,060
5	2240	14,616
6	3612	22,304
7	9090	54,294
8	23,368	133,964

forces are included in the problem by providing lid driven velocity of magnitude whereas all the other extremities are kept at rest. Square cylinder is placed at centre of enclosure and cold and adiabatic thermal distributions are maintained at the surface of square cylinder. Whereas, non-uniform boundary constraint is implemented at base wall of enclosure to remove thermal singularity. Boussinesq approximation is utilized to cater the density fluctuation with respect to temperature. The density variations are small up to moderate with temperature so the approximation is fair enough to simulate the results.

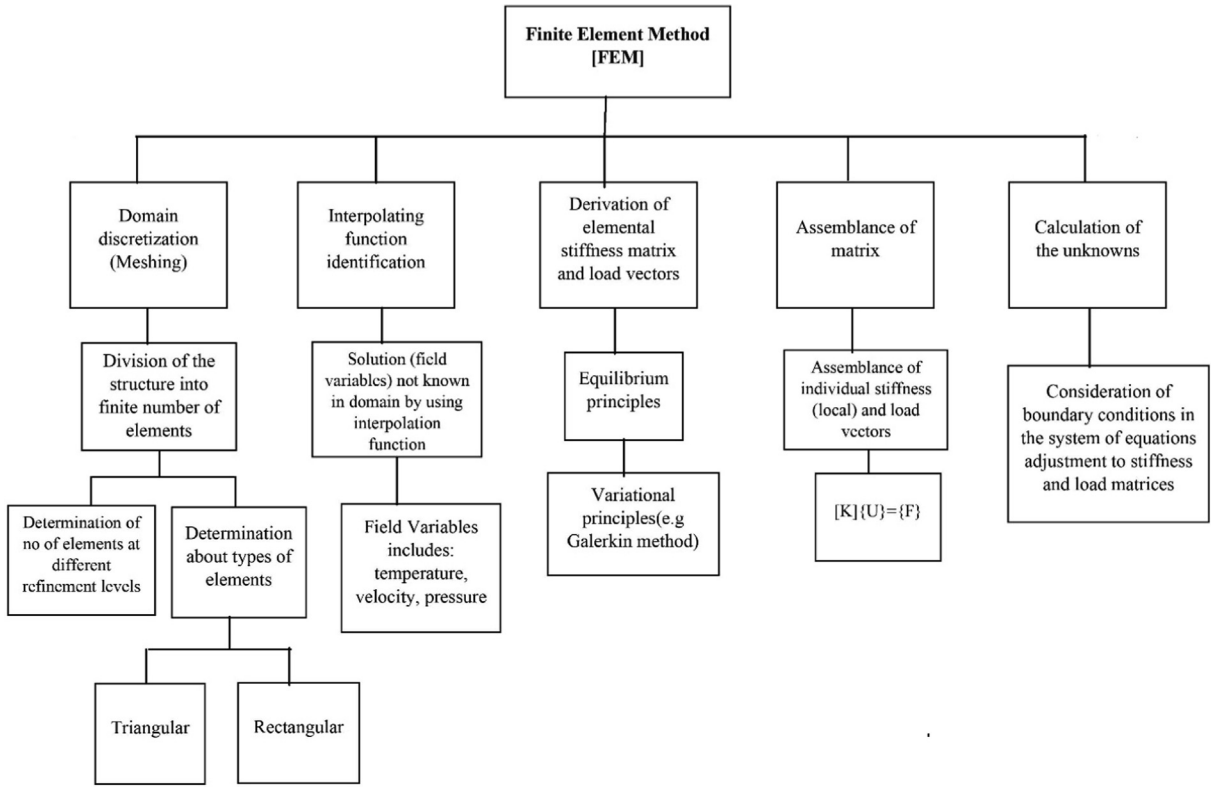


Fig. 3 Schematic diagram of finite element method.

The constitutive governing mass, momentum and energy equations are expressed as under [8].

$$\bar{U}_X + \bar{V}_Y = 0, \quad (1)$$

$$\bar{U}\bar{U}_X + \bar{V}\bar{V}_Y = -\frac{1}{\rho}\bar{P}_X + v(\bar{U}_{XX} + \bar{U}_{YY}), \quad (2)$$

$$\bar{U}\bar{V}_X + \bar{V}\bar{V}_Y = -\frac{1}{\rho}\bar{P}_Y + v(\bar{V}_{XX} + \bar{V}_{YY}) + g\beta(T - T_c), \quad (3)$$

$$\bar{U}\bar{T}_X + \bar{V}\bar{T}_Y = \alpha(\bar{T}_{XX} + \bar{T}_{YY}), \quad (4)$$

subjected to the velocity boundary conditions

$$\left. \begin{aligned} \bar{U}(X, L) = 1, \bar{U}(X, 0) = \bar{U}(0, Y) = \bar{U}(L, Y) = 0 \\ \bar{V}(X, 0) = \bar{V}(X, L) = \bar{V}(0, Y) = \bar{V}(L, Y) = 0 \end{aligned} \right\}, \quad (5)$$

thermal boundary constraints are as follows

$$\bar{T}(X, 0) = 1, \bar{T}(0, Y) = 0 = \bar{T}(L, Y), \frac{\partial \bar{T}}{\partial Y}(X, L) = 0, \quad (6)$$

$$\bar{T}(X, 0) = \sin\left(\frac{\pi X}{L}\right), \bar{T}(0, Y) = 0 = \bar{T}(L, Y), \frac{\partial \bar{T}}{\partial Y}(X, L) = 0. \quad (7)$$

Boundary conditions at surface of square cylinder

$$\left. \begin{aligned} \bar{U} = \bar{V} = \bar{T} = 0, \quad \text{for cold cylinder} \\ \bar{U} = \bar{V} = \frac{\partial \bar{T}}{\partial n} = 0 \quad \text{for adiabatic cylinder} \end{aligned} \right\}. \quad (8)$$

Table 2 Code validation for local Nusselt number against (Re) without obstacle.

Re	100	400	1000
Present	2.0399	4.0992	6.6309
Mehmood et al. [20]	2.0300	4.0700	6.5800
Astanina et al. [14]	2.0500	4.0900	6.7000

Table 3 Code validation for local Nusselt number against (Re) with obstacle.

Ri	Present	Mehmood et al. [29]	Akand et al. [16]
0.1	5.4611	5.5317	5.6118
1.0	5.4957	5.5684	5.6935
10	7.7951	7.9029	7.9083

Here, \bar{T} represents the temperature, α shows thermal diffusivity and v signifies kinematic viscosity while \bar{p} be the pressure, ρ be the density, the temperature at the cold and hot wall are defined by T_h and T_c .

Following transformation are used to non-dimensionalized governing equations attained in Eqs. (2)–(4).

$$x = \frac{X}{L}, y = \frac{Y}{L}, u = \frac{\bar{U}}{U_{Lid}}, v = \frac{\bar{V}}{U_{Lid}}, p = \frac{\bar{P}}{\rho U_{Lid}^2}, \theta = \frac{\bar{T} - \bar{T}_c}{\bar{T}_h - \bar{T}_c}$$

The reduced non-dimensionalized form of constitutive equations are as under referred to [8].

Table 4 A comparison of the Local Nusselt number at three different meshing levels against Pr.

Pr	Nu_{Local}		
	200×200	300×300	400×400
0.015	1.9787	1.9790	1.9785
0.7	2.4155	2.4149	2.4156
5.0	3.9810	3.9812	3.9808

$$u_x + v_y = 0, \quad (9)$$

$$uu_x + vv_y = -p_x + \frac{1}{Re}(u_{xx} + u_{yy}), \quad (10)$$

$$uv_x + vv_y = -p_y + \frac{1}{Re}(v_{xx} + v_{yy}) + Ri \times \theta, \quad (11)$$

$$u\theta_x + v\theta_y = \frac{1}{PrRe}(\theta_{xx} + \theta_{yy}), \quad (12)$$

Associated momentum boundary constraints in non-dimensionalized form are given by.

$$\left. \begin{aligned} u(x, 1) = 1, u(x, 0) = u(0, y) = u(1, y) = 0 \\ v(x, 0) = v(x, 1) = v(0, y) = v(1, y) = 0 \end{aligned} \right\} \quad (13)$$

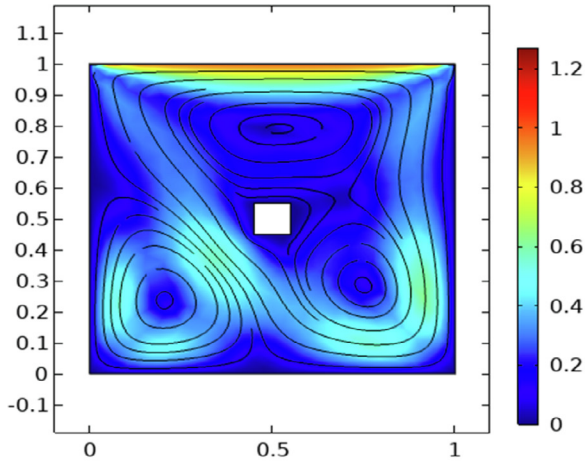
Associated thermal boundary constraints in non-dimensionalized form for uniform case

$$\theta(x, 0) = 1, \theta(0, y) = 0 = \theta(1, y), \frac{\partial \theta}{\partial y}(y, 1) = 0, \quad (14)$$

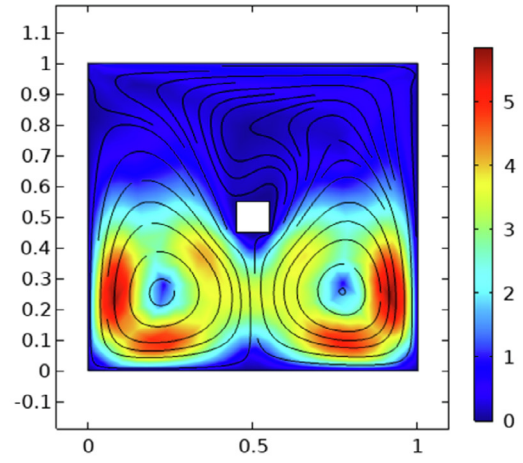
$$\theta(x, 0) = \sin(\pi x), \theta(0, y) = 0 = \theta(1, y), \frac{\partial \theta}{\partial y}(x, 1) = 0, \quad (15)$$

boundary conditions for the cylindrical blockage in non-dimensionalized form is shown as under.

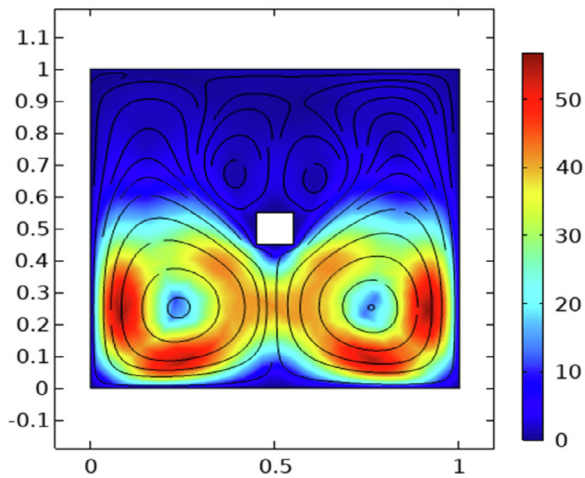
$$\left. \begin{aligned} u = v = \theta = 0, \quad \text{for the cold cylinder} \\ u = v = \frac{\partial \theta}{\partial n} = 0 \quad \text{for adiabatic cylinder} \end{aligned} \right\} \quad (16)$$



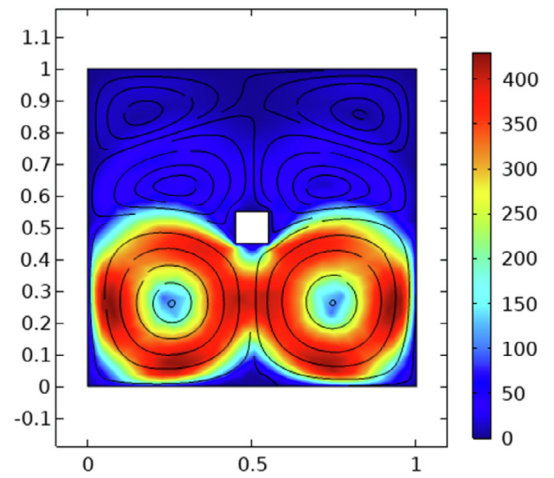
(a) $Gr = 10^3$



(b) $Gr = 10^4$



(c) $Gr = 10^5$



(d) $Gr = 10^6$

Fig. 4 Influence of Gr on streamlines with uniform heated bottom wall: cold cylinder case, $Pr = 0.015$ and $Re = 1$.

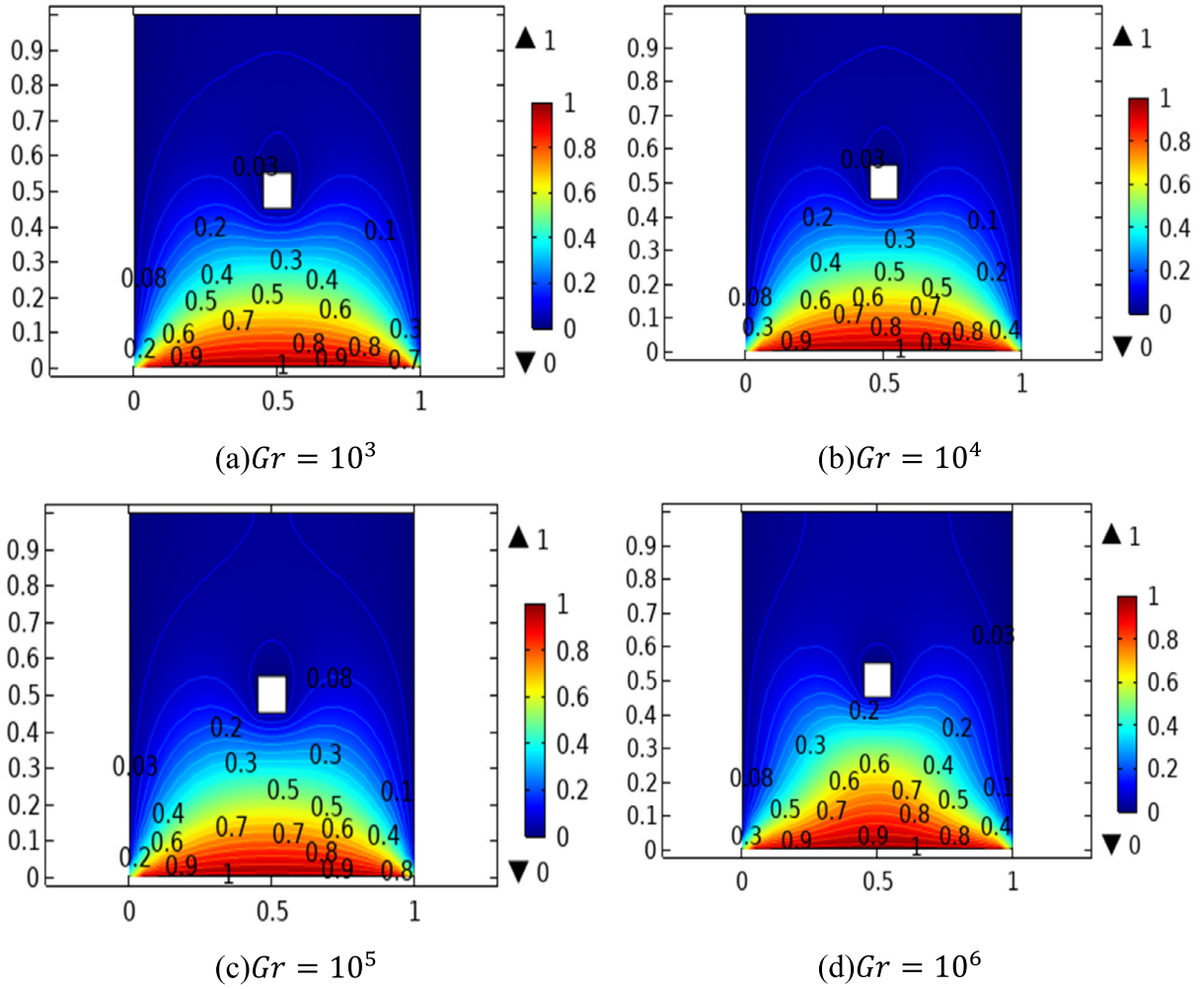


Fig. 5 Influence of Gr on isotherms with uniform heated bottom wall: cold cylinder case, $Pr = 0.015$ and $Re = 1$

The non-dimensional parameters appeared as a result of the transformation giving rise to non-dimensional system are $Re = \frac{U_{lid} L}{\nu}$, $Gr = \frac{g\beta(T_h - T_c)L^3}{\nu^2}$ and $Pr = \frac{\nu}{\alpha}$ respectively. Another important dimensionless parameter that gives importance of free versus forced convection is the Richardson number expressed as $Ri = \frac{Gr}{Re^2}$. For the cases in which $Ri \gg 1$, flow is dominated by buoyancy and hence a regime of natural convection dominates and for the cases $Ri \ll 1$ flow is forced convection dominant due to the shearing effects of the boundaries and a regime of forced convection prevails. However, both the natural and forced convection are comparable for the situations when $Ri \approx 1$ leading to a regime of mixed convection.

Nusselt number is also computed as post processing using $Nu = \frac{\partial \theta}{\partial n}|_{wall}$ and $Nu_{avg} = \frac{1}{L} \int_0^L Nu ds$.

3. Numerical scheme and solvers

Fluid flow behaviour in non-confined boundaries is easily handled by way of exact approaches but extracting the solution in closed enclosure along with various shapes of obstacle is difficult with the help of traditional methods. So, most of the researchers utilize numerical schemes to report the findings and most generous methods are FDM, FEM and FVM.

Among these mentioned numerical methodologies finite element scheme is a versatile method because of the fact that the modelling of complex and irregular shapes is easily handled by discretizing the available domain with finite elements. We have utilized the stable quadratic elements for the computations of velocity and temperature whereas the pressure is approximated through linear elements. In present pagination a hybrid finite element mesh is used consisting of rectangular and triangular elements. The computational mesh at coarse grid level is disclosed in Fig. 2 and the corresponding degrees of freedom at further refinement levels are shown in Table 1. Steps involving in finite element method are mentioned in Fig. 3. In FEM Newton's scheme is capitalized for linearization of non-linearized expressions and resulting linear system of equations is heeded through a direct solver based on elimination with special rearrangement of unknowns. The following convergence criterion is set for the nonlinear iterations.

$$\left| \frac{\chi^{n+1} - \chi^n}{\chi^{n+1}} \right| < 10^{-6}$$

where χ characterizes the general solution component.

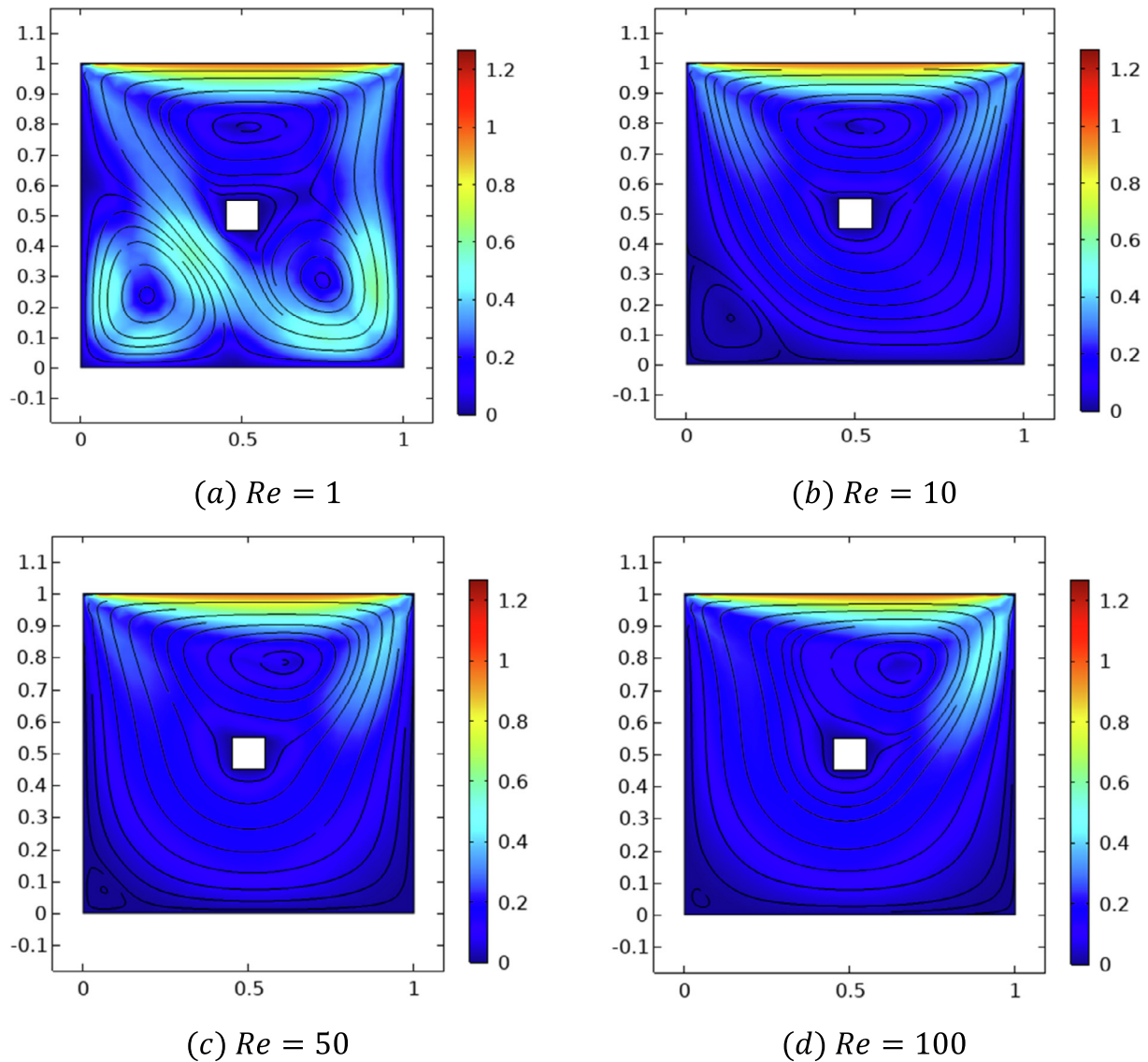


Fig. 6 Influence of Re on streamlines with uniform heated bottom wall: cold cylinder case, $Pr = 0.015$ and $Gr = 10^3$

4. Results and interpretation

The segment is disclosed the influence of involved physical parameters on concerning distributions generated due to accounting the aspect of mixed convection in viscous fluid in square cavity. Formulation of problem is conceded in the form of partial differential system in dimensionless form. Stream lines and isotherms patterns are drawn to envisage deviation in distributions. FEM based commercial software is utilized to find results.

4.1. Code Validation

Assurance about convergence of numerical simulation to accurate results, the size of grid has been maximized against independent grid size. Validation about code is obtained in [Table 2](#) and [Table 3](#) for finding local Nusselt number without and with obstacle respectively. A complete agreement is found with results accessed in [\[14,16,29\]](#).

4.2. Grid independence test

Validation of computational scheme has been tested by showing grid size independence test in which Local Nusselt number is computed against (Pr) by varying its range from and by fixing $Gr = 10^3$ and $Ri = 0.01$ for non-uniform heating case. It is noticed that a grid resolution of 300×300 is fine enough for grid independency therefore all the simulations are performed at this grid number which is fine level of meshing. In addition, an observation about computation of Nusselt number at finer level is concerned the results are matching with previous level. So, in view of saving computational and time cost the variation in flow characteristic against involved parameters are observed at Coarse level (see [Table 4](#)).

5. Further parametric study and graphical outcomes

[Figs. 4–5](#) exhibit streamlines and isotherms for the uniformly heated base by fixing Pr and Re but for changing Gr . In [Fig. 4\(-](#)

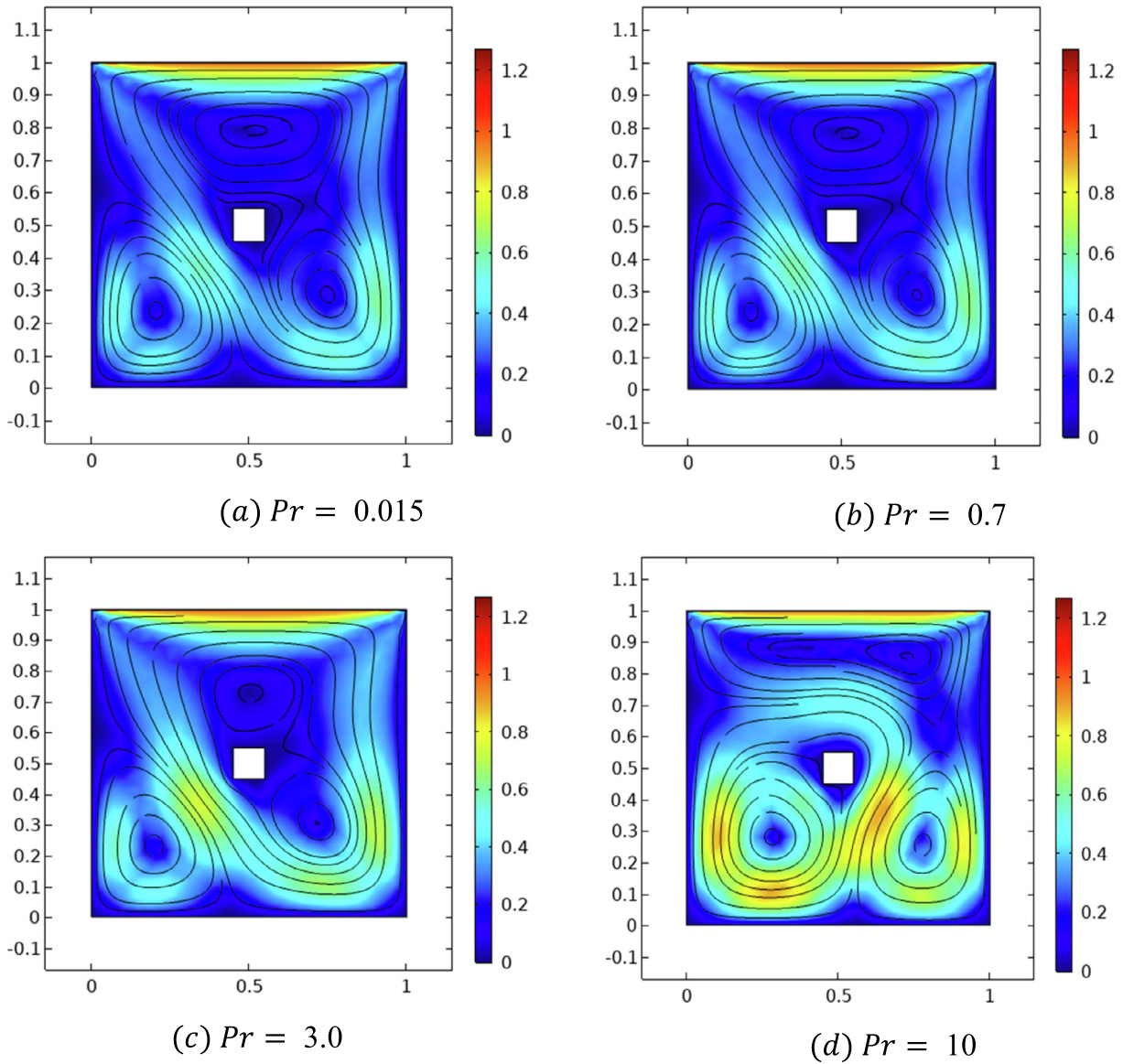


Fig. 7 Influence of (Pr) on streamlines with uniform heated bottom wall: cold cylinder, $Re = 1$ and $Gr = 10^3$

a-d) it is observed at lower magnitude of Gr i.e. $Gr = 10^3$ the effect of forced convection generated due to inertial forces generated in domain because of provision of lid driven velocity at upper boundary. So, in Fig. 4(a) clockwise rotation dominates the anticlockwise rotation and streamlines are not symmetric about centre and is inclined towards upper wall. In addition, it is seen that secondary vortex generated near lower corner left wall is squeezed. Whereas, in Fig. 4(b-d) it is observed that by increasing (Gr) the influence buoyancy forces enhances and more temperature difference is generated between cold and hot regions. It is because of the fact that (Gr) is the ratio of buoyancy to inertial forces so by increasing (Gr) temperature gradient enriches. It is also evidenced that by increasing (Gr) the amount of flow circulation enhances which is proved by observing Fig. 4(d). Subsequently, it is evaluated that with the gradual uplift in Gr , the buoyancy effects become more prominent due to which finally the clockwise and anticlockwise circulation becomes symmetrical at $Gr = 10^6$.

Fig. 5(a-d) illustrates the change in magnitude of isotherms against (Gr) ranging from $Gr = 10^2 - 10^6$ in the presence of cold cylinder in the centre. It is observed that by increasing magnitude of Grashof number (Gr) temperature difference elevates from bottom wall towards cylinder. Since, (Gr) is the ratio of buoyancy driven to viscous forces mathematically represented in the form $Gr = \frac{g\beta(\tilde{T}_h - \tilde{T}_c)L^3}{\nu^2}$ so by increasing (Gr) viscous forces reduces due to which average kinetic energy of fluid molecules enhances and thus temperature uplifts. In addition, it is also depicted that due to the presence of cold blockage more isotherms are accumulated in lower portion of the cavity. Due to more diffusion at $Gr = 10^6$ more deformation in parabolic shape is attained.

Variation in stream lines against increasing magnitude of Reynolds number (Re) is envisioned in Fig. 6(a-d). From the attained snapshots it is visualized that by increasing (Re) the magnitude of force convection enhances and become dominant

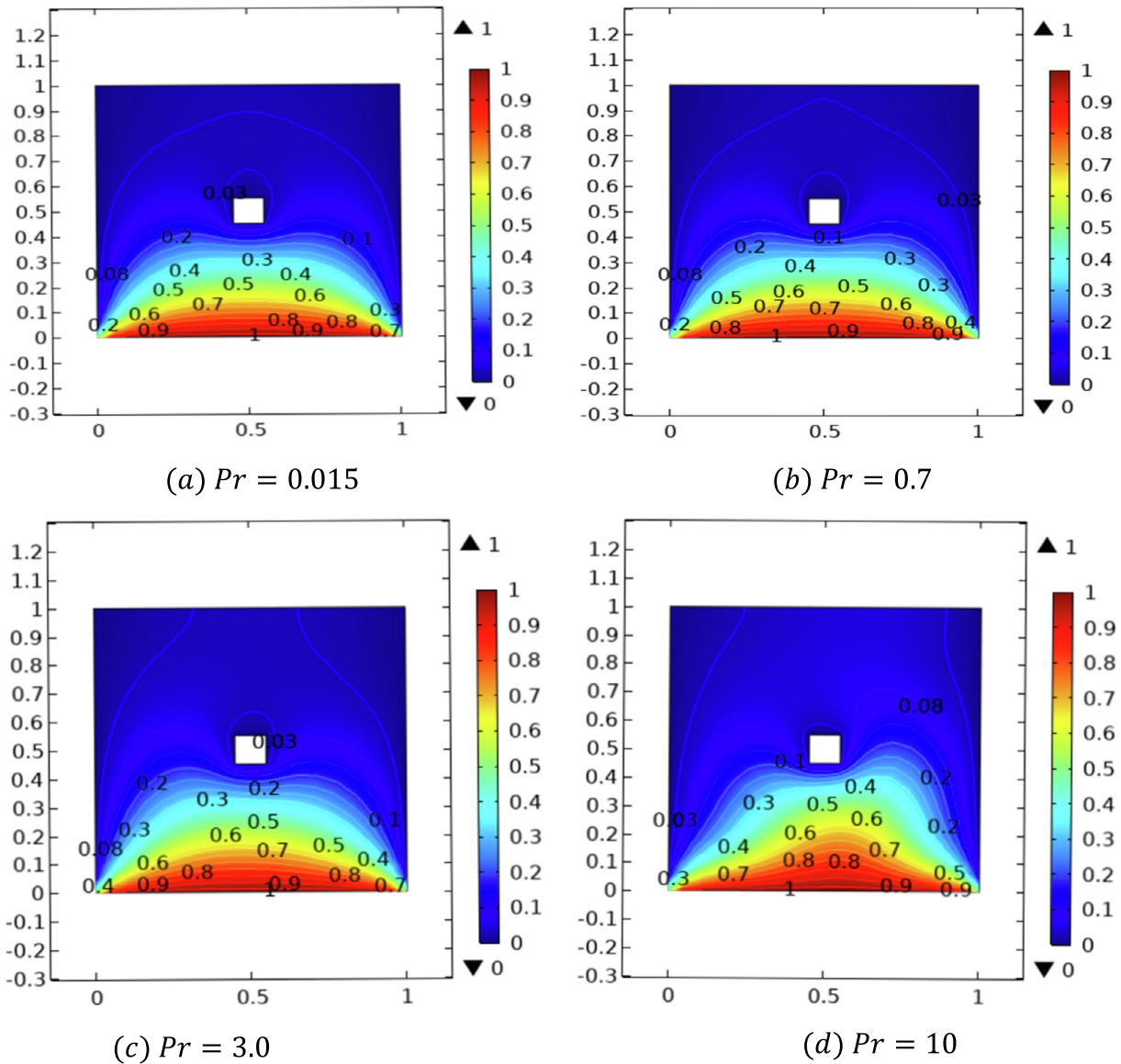


Fig. 8 Influence of Pr on isotherms with uniform heated bottom wall: cold cylinder case $Re = 1$ and $Gr = 10^3$

over natural convection. Since, force convection is generated due to movement of upper lid so slip velocity impressively effect the motion which is observed from vortices formation. One can also notice that strength of clockwise rotation increases with an increase in Re as expected due to dominance over natural convection. Furthermore, the right secondary vortex disappears at higher Reynolds numbers.

Variation in streamlines against different magnitudes of (Pr) is explicated in Fig. 7. It can be explicitly seen that by increasing (Pr) momentum diffusivity of fluid molecules increases due to which more circulations are generated at higher magnitude of (Pr). In addition, it is also observed that secondary vortex is located at lower corner of left wall at lower magnitude of (Pr) whereas, it shows migration towards center at $Pr = 10$. It is justified by the fact that (Pr) signifies ratio of momentum to thermal diffusivity so by growing the value of Pr motion generated by the movement of upper wall is dom-

inant and is transferred quickly towards the lower portion of cavity.

Fig. 8 exhibits the influence of (Pr) on temperature field by considering uniform heated bottom wall with cold cylinder via isothermal plots. From the adorned sketches it is divulged that the magnitude of heat increases with (Pr) because it generates viscous diffusion and more heat is transferred from base wall. It is also noteworthy that the symmetry of isotherms is disturbed for high values of (Pr).

In Fig. 9 we investigated the effect of $Gr = 10^3 - 10^6$ on streamlines. Since the velocity in cavity is generated by moving upper wall of cavity so by increasing Gr the fluid moves more extensively down side which can be justified from the circulations. The enhancement in the magnitude of flow with growth in Gr is because of fact that by incrementing Gr viscosity reduces and less resistance is provided to fluid molecules at high Gr .

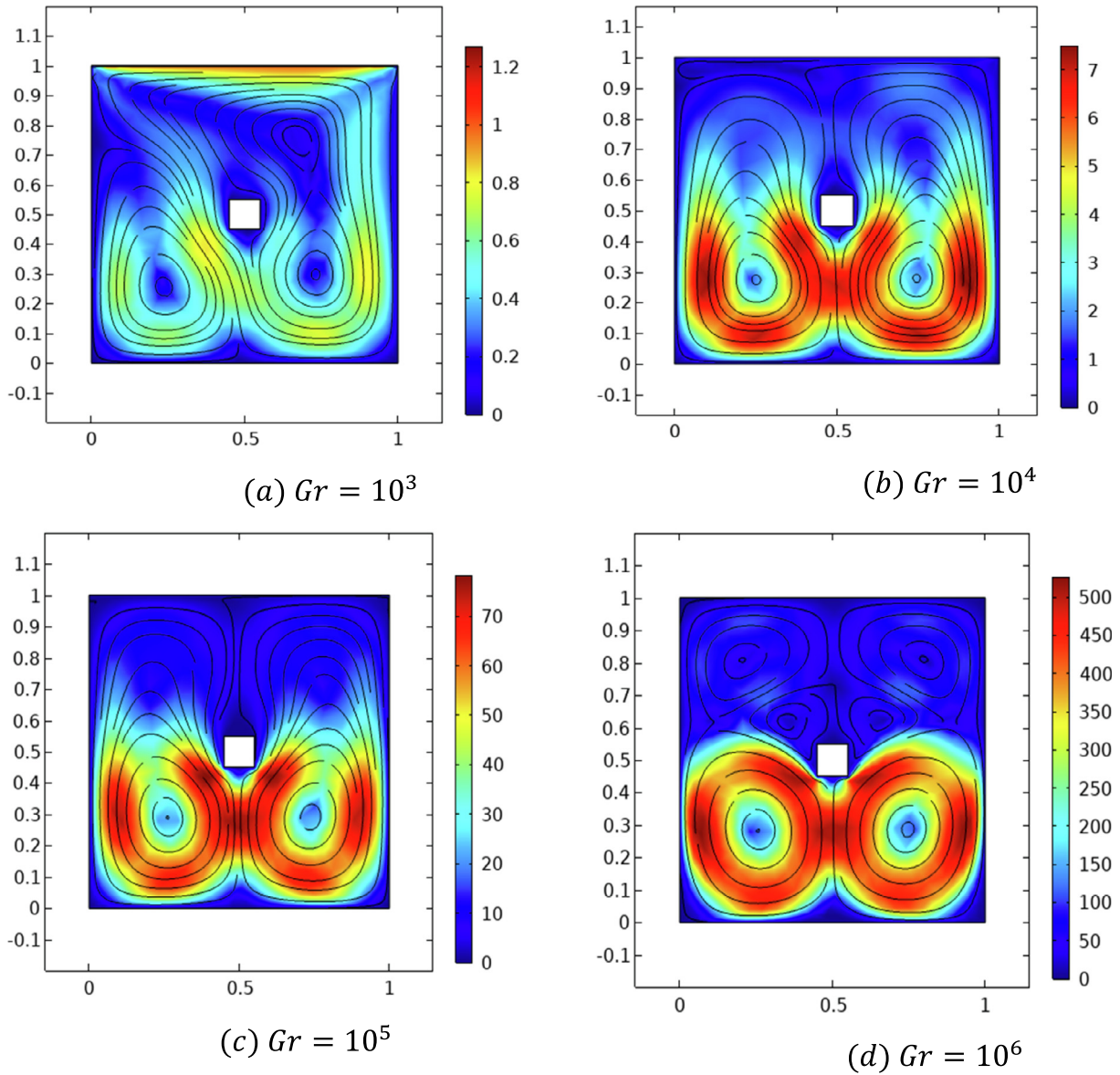


Fig. 9 Influence of Gr on streamlines with non-uniform heated bottom wall: adiabatic cylinder with $Pr = 0.015$ and $Re = 1$.

Isotherms for non-uniform bottom heating by varying $Gr = 10^3 - 10^6$ are interpreted in Fig. 10. It is demonstrated that with increment in Gr isotherms intensity increases and also the symmetry of curves disturbs. It is because by incrementing Gr the temperature difference between cold and hot region grows and heat diffuses quickly. It is worthwhile to mention that thermal singularity is produced in temperature field for uniformly heated wall in contrast to non-uniform heating.

Analysis regarding the impact of (Re) on velocity field through stream lines is seen in Fig. 11. It is portrayed that at low magnitude i.e. $Re = 1$ the anticlockwise rotation representing natural convection is more visible, however this circulation region is shortened for other higher magnitude of Re . It is because of the fact that at $Re = 1$ the influence of viscous diffusion and thermal diffusion balances each other whereas if we increase magnitude of Re gradually from $Re = 10 - 100$ the role of viscous diffusion enriches so thus viscosity effect does not allow fluid to accelerate.

To illustrate the deviation in velocity with (Pr) Fig. 12 is illuminated. It is seen that by increasing (Pr) the magnitude of velocity near obstacle increases. In addition, it is observed that for lower magnitude of (Pr) the shape of secondary vortex squeezes. It is because by increasing (Pr) momentum diffuses more dominantly within the cavity in comparison to the lower magnitude of (Pr) because of increase of viscous diffusion.

The impact of Prandtl number from lower to higher values on isotherms for adiabatic cylinder with non-uniformed heating is shown in Fig. 13. It is seen that by increasing (Pr) heat transfer generated by non-uniform heating at base wall reduces. In addition, it is also observed that for lower values of (Pr), the isotherms are symmetric with respect to centre, however at high (Pr), the isotherms are intensified towards wall. This behaviour is validated by the ratio of Prandtl number (Pr) which is the ratio of momentum to thermal diffusivity. So, by increasing (Pr) thermal diffusion enhances.

In Fig. 14, we have plotted the local Nusselt number with respect to (Pr) and (Gr) at $Re = 100$. For small magnitude

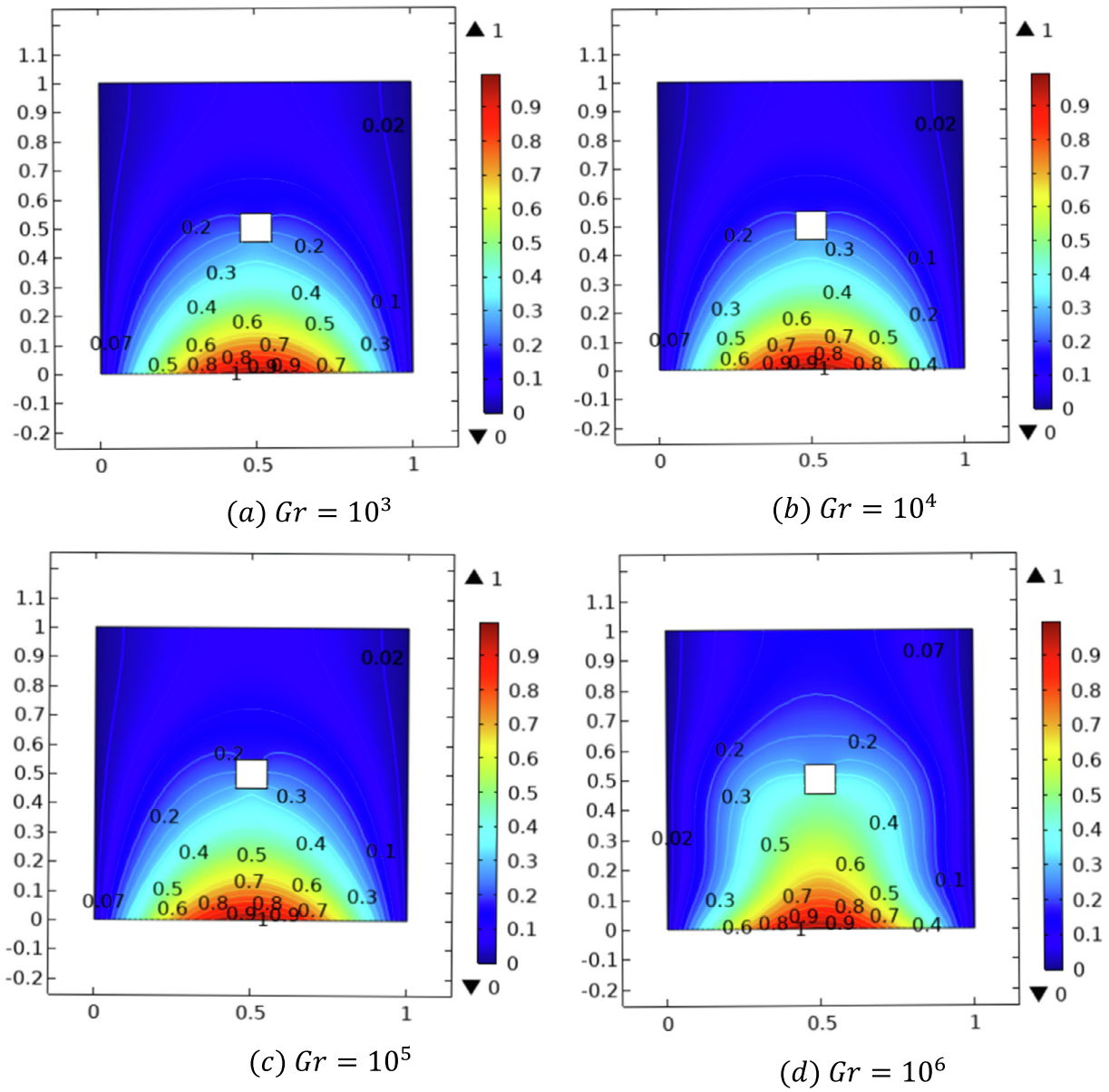


Fig. 10 Influence of Gr on isotherms with non-uniform heated bottom wall: adiabatic cylinder with $Pr = 0.015$, $Re = 1$.

of $Pr = 0.015$, the heat transfer coefficient is maximum whereas minimum magnitude is attained for $Pr = 10$. In view of effect of Grashof number (Gr) on heat flux coefficient it is manifested that by increasing (Gr) heat flux enhances due to enhancement in temperature difference between base wall and cylinder.

Fig. 15 provides the information about the change in Nu_{local} against increasing (Gr) and (Pr) for uniform heating of base wall. Here, it is manifested that for low magnitude of (Gr) and (Pr) no significant change in Nusselt number is seen. Whereas, for higher values of (Gr) significant increase in Nu_{local} is disclosed. Its due to the fact that by increasing (Gr) impact of buoyancy forces mounts as a consequence motion of fluid particles enriches and more heat is transferred from heated wall to other portions of enclosure.

Additionally, we have also computed a global quantity which is also served as a benchmark quantity for driven cavity

flows. Computation of kinetic energy is enumerated in **Table 5** for configuration of adiabatic square block against Re at $Pr = 0.015$, $Gr = 10^3$. Decreasing trend in kinetic energy is noticed for increasing magnitude of Re . This pattern is due to the fact that higher Re gives rise to vortices and flow is separated into different circulation zones.

Variation in Nusselt number at base wall against Grashof number (Gr), Richardson number (Ri) and Prandtl number (Pr) for uniform and non-uniform heating cases are enumerated in **Table 6**. It is disclosed that more heat is generated in case of uniform heating instead of non-uniform heating due to which thermal singularity is generated for uniformly heated distribution. The variation in Richardson expresses three different cases i) for $Ri \gg 1$, flow is dominated by regime of natural convection ii) for the $Ri \ll 1$ flow is forced convection dominant. However, both the natural and forced convection are comparable for the situations when $Ri \approx 1$ leading to a

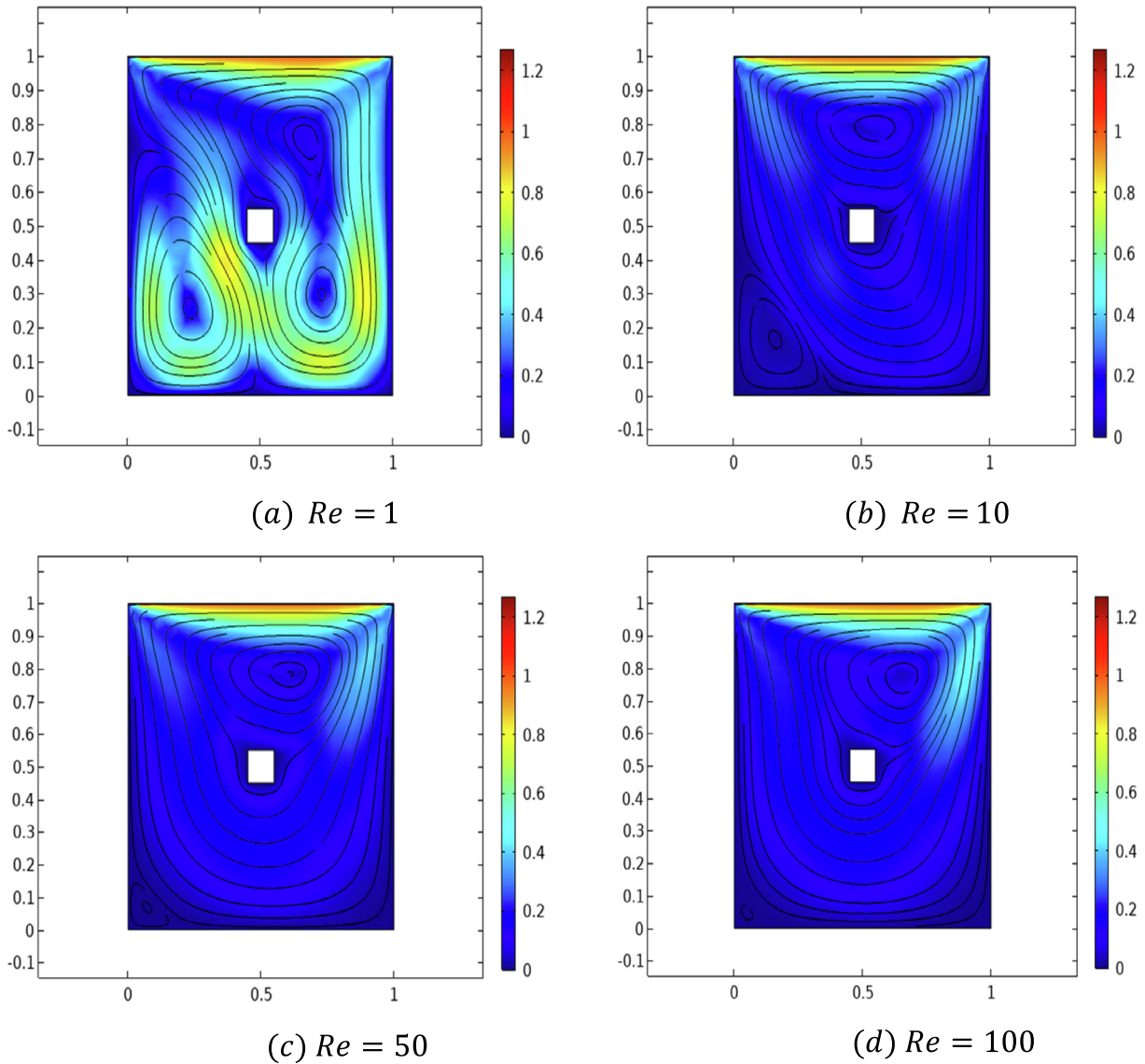


Fig. 11 Influence of Re on streamlines with non-uniform heated bottom wall: adiabatic cylinder with $Pr = 0.015$, $Gr = 10^3$.

regime of mixed convection. So, this table comprehensively discusses the variation in heat flux coefficient for all mentioned three regimes. Change in average Nusselt number at heated base wall against Grashof number (Gr), Prandtl number (Pr) in comparative manner for uniform and non-uniform heating distributions are displayed in Fig. 16. It is found that heat flux in case of uniform heating is dominant than non-uniform heat-

ing. In addition, it is depicted that heat transfer rate enhances against Prandtl number (Pr) for both considered thermal distributions. The reason behind this fact is that by increasing (Pr) momentum diffusivity of fluid enhances due to which kinetic energy as well as the temperature in the domain also uplifts. Thus, as an outcome elevated heat transfer rate is attained at higher magnitude of Pr .

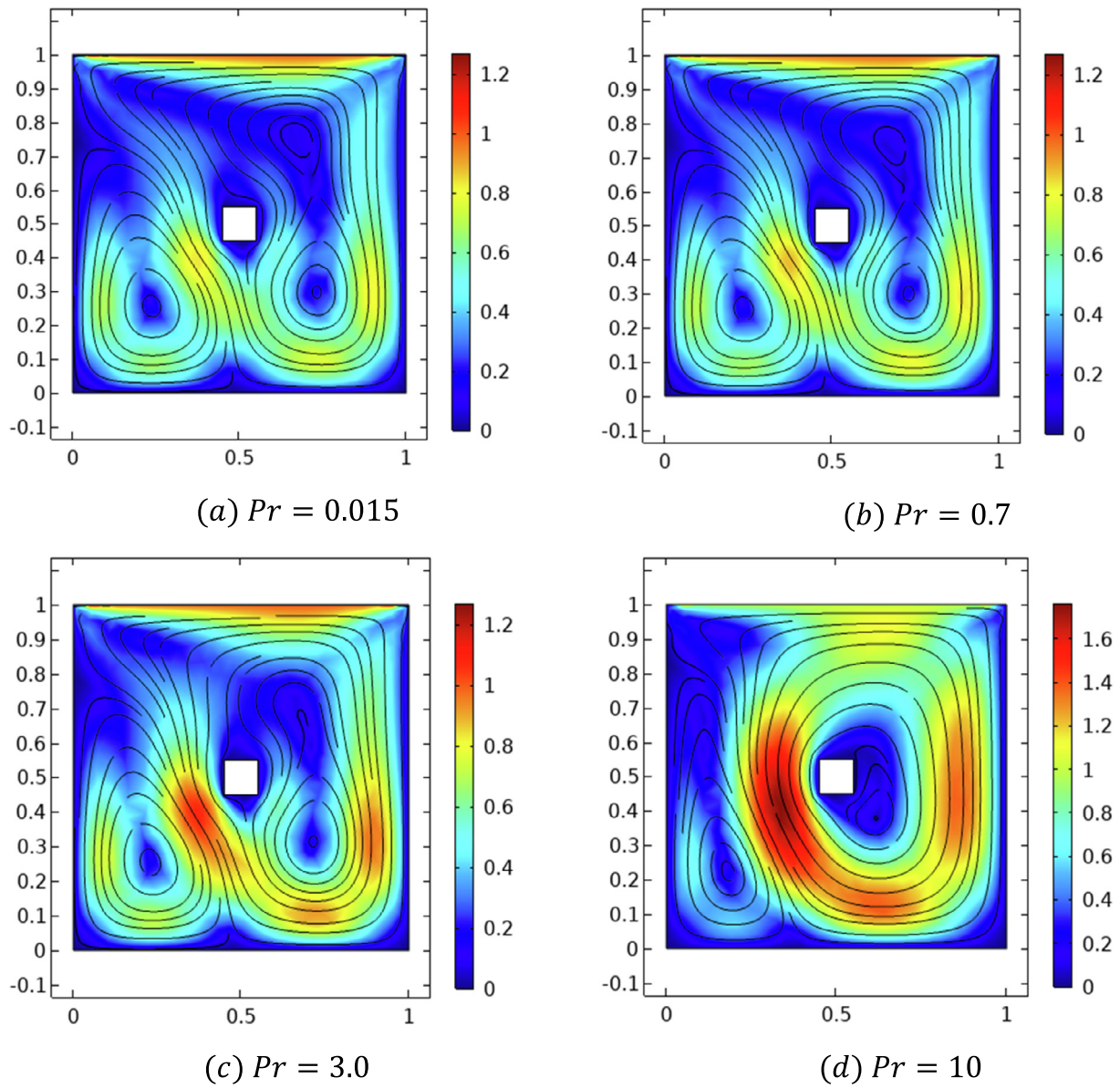


Fig. 12 Influence of Pr on streamlines with non-uniform heated bottom wall: adiabatic cylinder with $Re = 1$, $Gr = 10^3$

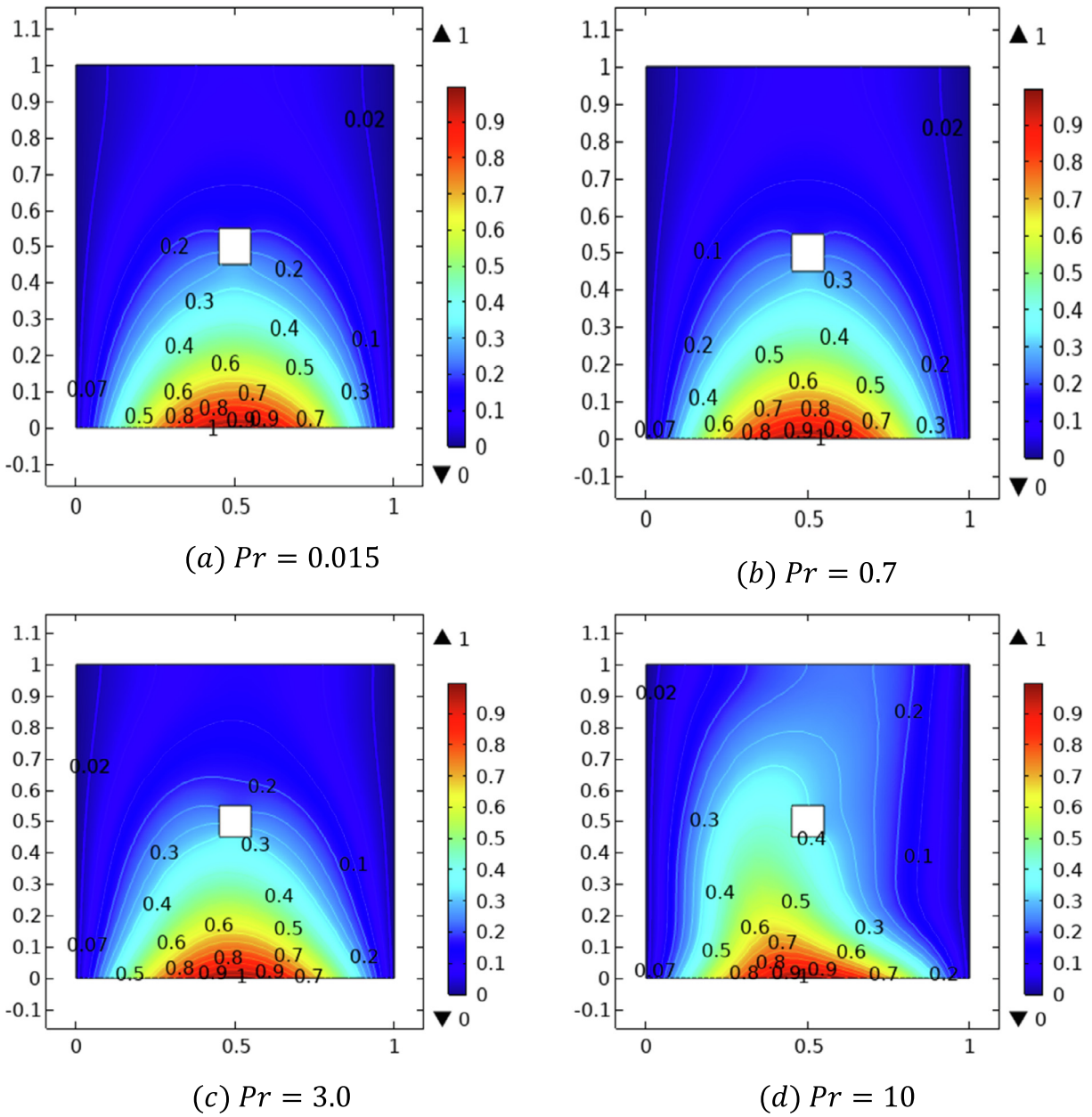


Fig. 13 Influence of (Pr) on isotherms with non-uniform heated bottom wall: adiabatic cylinder with $Re = 1, Gr = 10^3$.

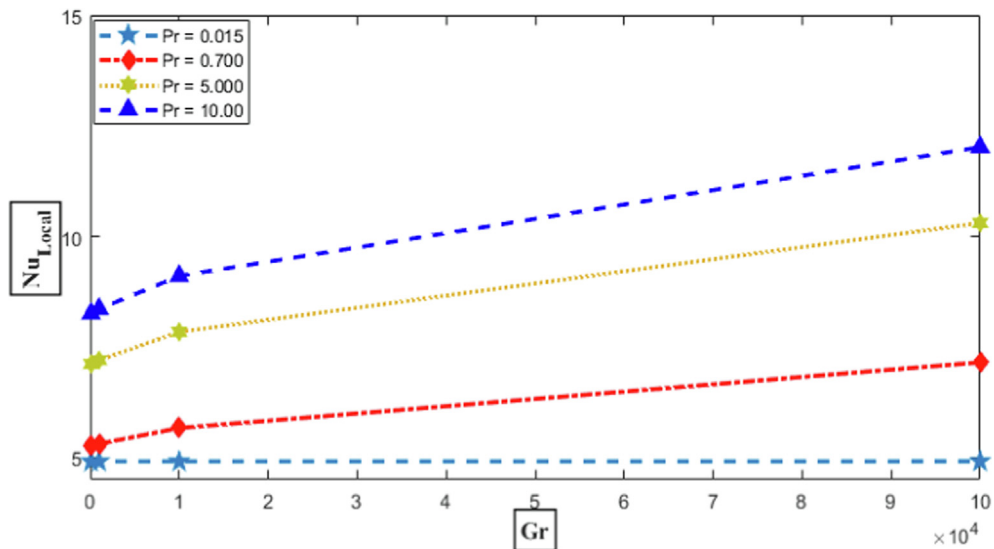


Fig. 14 Variation in Nu_{Local} for uniformly heated bottom wall against (Gr) and (Pr).

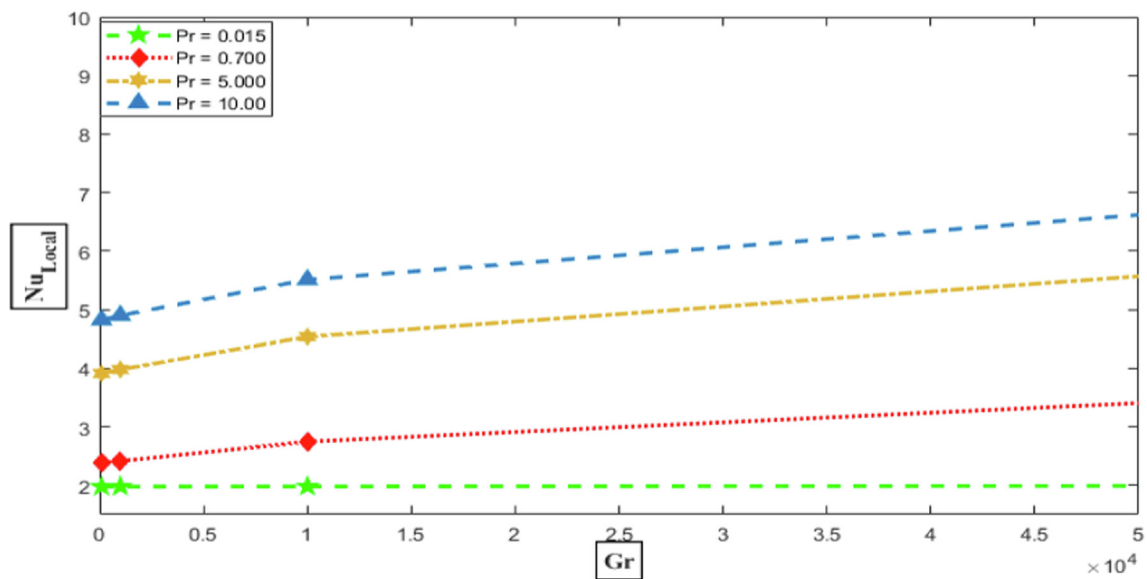


Fig. 15 Variation in Nu_{Local} for non-uniform bottom heated wall against (Gr) and (Pr).

Table 5 Variation in K.E. against Re and by fixing $Pr = 0.015, Gr = 10^3$.

Re	$K.E$
10	0.033923847
20	0.032846100
30	0.032107234
40	0.031412376
50	0.030728584
60	0.030062071
70	0.029428688
80	0.028846019
90	0.028328941
100	0.027888360

6. Conclusions

Mixed convective flow regime in viscous fluid flow in square enclosure for uniform and non-uniform thermal distributions along with consideration of cold and adiabatic cylinder was analysed in current communication. Mathematical formulation of problem by capitalizing governing law was executed in the form of dimensionless partial differential system. Numerical simulations were performed by applying the finite element procedure. Variation in associated momentum and temperature distributions in view of stream lines and isothermal patterns were disclosed. Quantities of engineering interest like kinetic energy, local heat flux coefficients was also measured

Table 6 Variation in Nu_{Local} for uniform and non-uniform heating bottom walls against (Gr), (Ri) and (Pr).

Gr	Ri	Pr	Uniform heated base wall Nu_{Local}	Non-uniformly heated base wall Nu_{Local}
10^2	0.01		4.9127	1.9785
10^3	0.10		5.0125	1.9787
10^4	1.00	0.015	5.1378	1.9810
10^5	10.0		4.9156	2.0047
10^6	100		5.2964	2.2535
10^2	0.01		5.2818	2.3807
10^3	0.10		5.3150	2.4155
10^4	1.00	0.700	5.6691	2.7463
10^5	10.0		7.1497	4.2310
10^6	100		10.681	8.1688
10^2	0.01		7.1161	3.9126
10^3	0.10		7.2045	3.9810
10^4	1.00	5.000	7.8467	4.5374
10^5	10.0		10.311	6.8574
10^6	100		13.859	9.9316
10^2	0.01		8.2599	4.8234
10^3	0.10		8.3655	4.9001
10^4	1.00	10.00	9.1092	5.5104
10^5	10.0		12.018	8.0090
10^6	100		14.438	9.3721

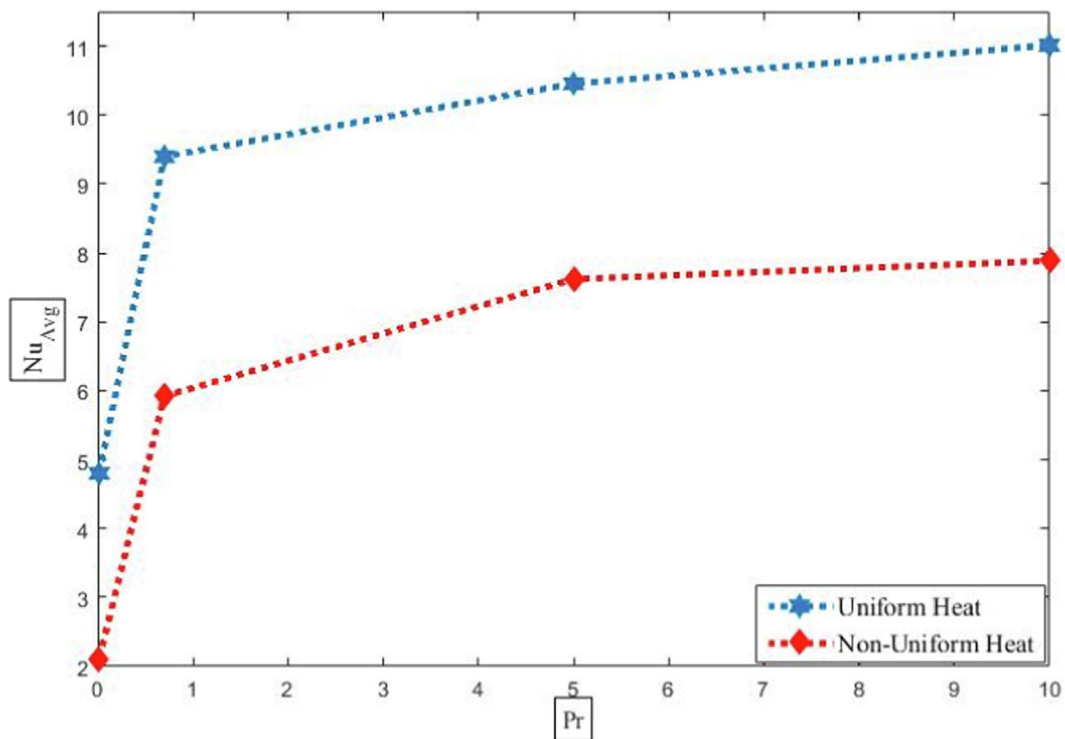


Fig. 16 Variation in Nu_{Avg} for Uniform and non-uniform bottom heated wall against (Gr) and (Pr).

against dimensionless involved physical parameters. Key findings of current analysis were enlisted below.

- (i) Heat flux in case of uniform heating at bottom wall is more than in the situation of non-uniform heating.
- (ii) Increase in Reynold number produces decrease in kinetic energy of fluid.

- (iii) Enhancement in Grashof number causes enrichment of thermal buoyancy forces due to which Nusselt number uplifts.
- (iv) Clock wise rotations increase against upsurge in magnitude of Reynold number which is evidenced form stream lines.

- (v) Squeezing of secondary vortex against Prandtl number arises due to dominance of viscous forces.
- (vi) This study reveals that obstacles of different shape having different thermal conditions plays effective role in handling of heat transfer characteristics.

Declaration of Competing Interest

The authors declare that they have no known competing financial interests or personal relationships that could have appeared to influence the work reported in this paper.

Acknowledgments

The authors express their appreciation to the Deanship of Scientific Research at King Khalid University for funding this work through research groups program under grant number R.G.P. 2/233/43. Emad E. Mahmoud acknowledges the Taif University Researchers Supporting Project number TURSP-2020/20, Taif University, Taif, Saudi Arabia.

References

- [1] O. Aydin, A. Unal, T. Ayhan, A numerical study on buoyancy-driven flow in an inclined square enclosure heated and cooled on adjacent walls, *Numer. Heat Transf. A*. 36 (1999) 85–599.
- [2] C.K. Cha, Y. Jaluria, Recirculating mixed convection flow for energy extraction, *Int. J. Heat Mass Transf.* 27 (1984) 1801–1810.
- [3] J. Imberger, P.F. Hamblin, Dynamics of lake reservoirs and cooling ponds, *A. Rev. Fluid Mech.* 14 (1982) 153–187.
- [4] F.J.K. Ideriah, Prediction of turbulent cavity flow driven by buoyancy and shear, *J. Mech. Eng. Sci.* 22 (6) (1980) 287–295.
- [5] L.A.B. Pilkington, Review lecture: the float glass process, *Proc. Roy. Soc. Lond.* 1A314 (1969) 1–25.
- [6] R. Schreiber, H.B. Keller, Driven cavity flows by efficient numerical techniques, *J. Comput. Phys.* 49 (2) (1983) 310–333.
- [7] M.C. Thompson, J.H. Ferziger, An adaptive multigrid technique for the incompressible Navier-Stokes equations, *J. Comput. Phys.* 82 (1) (1989) 94–121.
- [8] T. Basak, S. Roy Sharma, Analysis of mixed convection flows within a square cavity with linearly heated side wall, *Int. J. Heat Mass Trans.*, 52 (2009) 2224–2242.
- [9] C. Nouar, Numerical solution for laminar mixed convection in a horizontal annular duct: temperature-dependent viscosity effect, *Int. J. Numer. Methods Fluids* 29 (7) (1999) 849–864.
- [10] M.K. Moallemi, K.S. Jang, Prandtl number effects on laminar mixed convection heat transfer in a lid-driven cavity, *Int. J. Heat Mass Transfer* 35 (8) (1992) 1881–1892.
- [11] A.K. Prasad, J.R. Koseff, Combined forced and Natural convection heat transfer in a deep lid-driven cavity flow, *Int. J. Heat Fluid Flow* 17 (5) (1996) 460–467.
- [12] A.A. Mohamad, R. Viskanta, Effects of upper lid shear on the stability of flow in a cavity heated from below, *Int. J. Heat Mass Transfer* 32 (1989) 2155–2166.
- [13] A. Al-Amiri, K. Khanafer, J. Bull, I. Pop, Effect of sinusoidal wavy bottom surface on mixed convection heat transfer in a lid driven cavity, *Int. J. Heat Mass Transfer* 50 (9-10) (2007) 1771–1780.
- [14] M.S. Astanina, M.A. Sheremet, H.F. Oztop, MHD natural convection and entropy generation of ferrofluid in an open trapezoidal cavity partially filled with a porous medium, *Int. J. Mech. Sci.* 48 (2018) 326–337.
- [15] K. Khanafer, S.M. Aithal, Laminar mixed convection flow and heat transfer characteristics in a lid driven cavity with a circular cylinder, *Int. J. Heat Mass Transf.* 66 (2013) 200–209.
- [16] A.A. Mohamad, R. Viskanta, Transient low Prandtl number fluid convection in a lid driven cavity, *Numer. Heat Transfer A*. 19 (1991) 187–205.
- [17] A.W. Islam, M.A.S. Sharif, E.S. Carlson, Mixed Convection in a lid driven square cavity with an isothermally heated square blockage inside, *Int. J. Heat Mass Transf.* 55 (2012) 5244.
- [18] A.J. Shkarah, M.Y. Bin Sulaiman, M.R. bin Hj Ayob, Analytical Solutions of Heat Transfer and Film Thickness with Slip Condition Effect in Thin-Film Evaporation for Two-Phase Flow in Microchannel, *Math. Probl. Eng.* 2015 (2015) 1–15.
- [19] A. Ayub, H.A. Wahab, S.Z.H. Shah, S.L. Shah, A. Darvesh, A. Haider, Z. Sabir, Interpretation of infinite shear rate viscosity and a nonuniform heat sink/source on a 3D radiative cross nanofluid with buoyancy assisting/opposing flow, *Heat Transfer* 50 (5) (2021) 4192–4232.
- [20] S. Chaudhuri, P. Sourick Sinha, M. Chakraborty, S. Das, B.D. Sahoo, Thermal characteristics of forced convection in combined pressure and shear-driven flow of a non-Newtonian third-grade fluid through parallel plates, *Heat Transfer* 50 (2021) 6737–6756.
- [21] S. Chaudhuri, S. Sahoo, Effect of the aspect ratio on the flow characteristics of magnetohydrodynamic (MHD) third grade fluid flow through a rectangular channel, *Sādhanā* 43 (2018) 106–120.
- [22] S.S. Shah, R. Haq, W.A. Kouz, Mixed convection analysis in a split lid-driven trapezoidal cavity having elliptic shaped obstacle, *Int. Commun. Heat Mass Transfer* 126 (2021) 105448.
- [23] M. Dzodzo, D. Dzodzo, Natural convection in enclosures containing lead-bismuth and lead, *Int. J. Comput. Methods* 27 (2001) 13–25.
- [24] C. Beckermann, S. Ramadhyani, R. Viskant, Natural convection flow and heat transfer between a fluid layer and a porous layer inside a rectangular enclosure, *J. Heat Transf.* 109 (1987) 363–370.
- [25] M.H. Ali, T. Ahmed, K.I. Hamada, Numerical Study of Non-Darcian Natural Convection Heat Transfer in a Rectangular Enclosure Filled with Porous Medium Saturated with Viscous Fluid, *Tikrit J. Eng. Sci.* 2 (2008) 90–111.
- [26] K.E. Torrance, J.A. Rockett, Numerical study of natural convection in an enclosure with localized heating from below creeping flow to the onset of laminar instability, *J. Fluid Mech.* 36 (1969) 33–54.
- [27] J. Shkarah, convective heat transfer and fully developed flow for circular tube newtonian and non-newtonian fluids condition, *J. Therm. Eng.* 7 (2021) 409–414.
- [28] K. Mehmood, S. Hussain, M. Sagheer, Mixed convection in alumina-water nanofluid filled lid driven square cavity with an isothermally heated square blockage inside with magnetic field effect, *Int. J. Heat Mass Transf.* 109 (2017) 397–409.
- [29] A. Ayub, H.A. Wahab, Z. Sabir, A. Arbi, A note on heat transport with aspect of magnetic dipole and higher order chemical process for steady micropolar fluid, *Computat. Overview Fluid Struct. Interaction* 97 (2021).
- [30] S.Z. Shah, H.A. Wahab, A. Ayub, Z. Sabir, Higher order chemical process with heat transport of magnetized cross nanofluid over wedge geometry, *Heat Transfer* 50 (2021) 3196–3219.
- [31] A. Ayub, H.A. Wahab, S.Z. Hussain Shah, Z. Sabir, On heated surface transport of heat bearing thermal radiation and MHD Cross flow with effects of nonuniform heat sink/source and buoyancy opposing/assisting flow, *Heat Transfer* 50 (2021) 6110–6128.
- [32] A. Ayub, H.A. Wahab, M. Balubaid, S.R. Mahmoud, R. Sadat, Analysis of the nanoscale heat transport and Lorentz force based on the time-dependent Cross nanofluid, *Eng. with Comput.* (2020) 1–20.

- [34] C.J. Chen, K.S. Ho, Finite analytical numerical solution of heat transfer in two dimensional cavity flow, *Numer. Heat Transfer* 4 (1981) 179–197.
- [35] K. Torrance, R. Davis, D. Gill, D. Gautam, A. Hsui, S. Lyons, H. Zien, Cavity flows driven by buoyancy and shear, *J. Fluid Mech.* 51 (1972) 221–231.
- [36] R. Iwatsu, J.M. Hyun, K. Kuwahara, Convection in a differentially heated square cavity with a torsionally oscillating lid, *Int. J. Heat Mass Transfer* 35 (1992) 1069–1076.
- [37] R. Iwatsu, J.M. Hyun, K. Kuwahara, Numerical simulation of flows driven by torsionally oscillating lid in a square cavity, *J. Fluids Eng.* 114 (1992) 143–151.
- [38] A.I. Alsabery, R. Mohebbi, A.J. Chamkha, I. Hashim, Effect of local thermal non-equilibrium model on natural convection in a nanofluid-filled wavy-walled porous cavity containing inner solid cylinder, *Chem. Eng. Sci.* 201 (2019) 247–263.
- [39] T. Tayebi, A.J. Chamkha, Entropy generation analysis due to MHD natural convection flow in a cavity occupied with hybrid nanofluid and equipped with a conducting hollow cylinder, *J. Therm. Anal. Calorim.* 139 (3) (2020) 2165–2179.
- [40] A.S. Dogonchi, M.A. Ismael, A.J. Chamkha, D.D. Ganji, Numerical analysis of natural convection of Cu–water nanofluid filling triangular cavity with semicircular bottom wall, *J. Therm. Anal. Calorim.* 135 (6) (2019) 3485–3497.
- [41] A. Dogonchi, T.A. Sattar, A.J. Chamkha, D.D. Ganji, Natural convection analysis in a cavity with an inclined elliptical heater subject to shape factor of nanoparticles and magnetic field, *Arabian J. Sci. Eng.* 44 (9) (2019) 7919–7931.